2018

Determination of the SIVmac Vif-Human APOBEC3B Interaction

Oumar Sanogo
Minnesota State University, Mankato

Recommended Citation

Determination of the SIVmac Vif-Human APOBEC3B Interaction

By

Oumar Sanogo

A Thesis Submitted in Partial Fulfillment of the

Requirements for the Degree of

Master of Science

In

Biology

Minnesota State University Mankato
Mankato, Minnesota
December 2018

Oct 11 2018

Determination of the SIVmac Vif-Human APOBEC3B
Interaction

Oumar Sanogo

This thesis has been examined and approved by the following
members of the student's committee.

_____Allison M. Land____
Advisor

_____Rachel Cohen_____
Committee Member

_____Timothy Secott____
Committee Member

Aknowlegdements:

Abstract:

Determination of the SIVmac Vif-Human APOBEC3B Interaction

Oumar Sanogo, M. S.
Minnesota State University Mankato
Mankato, Minnesota
2018

The APOBEC3 family of enzymes are DNA cytosine deaminases, some of which restrict replication of HIV-1. This viral restriction is caused by deamination of cytosines to uracils in the viral cDNA, resulting in lethal mutation. HIV-1 counteracts this deamination by producing the protein Vif, which targets the restricting APOBEC3 enzymes for proteosomal degradation. Previous studies have demonstrated that HIV-1 Vif mediates degradation of APOBEC3D (A3D), APOBEC3F (A3F), APOBEC3G (A3G), and APOBEC3H (A3H). Other lentiviruses may also encode a Vif protein, however not all Vif proteins can degrade the same APOBEC3 proteins. For example, SIVmac (simian immunodeficiency virus that infects rhesus macaques) Vif was reported to mediate degradation of APOBEC3B (A3B), but not A3F. A3B does not restrict HIV, but is highly expressed in multiple cancers (bladder, cervical, lung squamous cell carcinoma, lung adenocarcinoma, head and neck, and breast) and is thought to contribute to tumor evolution. My goal is to determine the binding region between SIVmac Vif and A3B.

To achieve this goal, structurally defined regions of the A3B protein were swapped with the analogous regions of A3F in an expression vector. These hybrid constructs were created by primer-directed mutagenesis. Once the sequence was confirmed, the vectors encoding hybrid A3B-A3F were co-transfected with SIVmac Vif into 293T cells, and then immunoblots of whole cell lysates were performed to determine the level of APOBEC3 degradation. Surprisingly, in our system we observed that both A3B and A3F were equally sensitive to SIVmac Vif-mediated degradation. Determining the binding region between SIVmac Vif and A3B is important for understanding this protein interaction. A3B is a significant biological target, as increased A3B expression is found in tumors and is hypothesized to accelerate the progression of cancer by increasing the rate of genomic mutation. SIVmac Vif, which has been determined to mediate the proteasomal degradation of A3B, could be used to develop cancer therapeutics that decrease tumor evolution by targeting A3B. In this study, SIVmac Vif degraded huA3B and rhA3F, and the huA3B-rhA3F α6 chimera. It was inferred that α6 helix in huA3B is an important determinant for the interaction with SIVmac Vif. This result can be studied further in order to create a model that describes the binding interface between SIVmac239 Vif and A3B, which will, ultimately, lead to creating a biochemical drug against the effect of misregulated A3B in cancer therapy.

TABLE OF CONTENTS

Introduction
HIV:

HIV (human immunodeficiency virus) is an enveloped lentivirus of the family

Retroviridae that infects cells of the human immune system, mainly $CD4^+$ T cells (1).

This results in an overall decreased immune response, including increased

susceptibility to specific cancers such as Kaposi sarcoma, non-Hodgkin's lymphoma,

cervical cancer, and anal cancer(2). There are two strains of HIV currently

circulating; HIV-1 is the major cause of the HIV pandemic, while HIV-2 infects a

smaller amount of people. Both viruses contain nine genes (HIV-1: gag, pol, env, vif,

tat, vpu, vpr, rev, nef; HIV-2: gag, pol, env, vif, tat, vpx, vpr, rev, nef) and are the

result of zoonotic transmission from an SIV (simian immunodeficiency viruses)

infected primate to a human. HIV-1 is believed to be the result of transmission from

a chimpanzee to a human, while HIV-2 was the result of transmission from a sooty

mangabey to a human(3).

The infectiousness of HIV is dependent on the susceptibility (host cell allows

adherence/entry of virus) and permissiveness (host cell allows replication of virus)

of the host cell. Adherence and entry of the virus to the host cell is facilitated by the

external glycoprotein (gp120) and the transmembrane glycoprotein (gp41) (1).

These viral glycoproteins form a complex (gp160), which interacts with the cellular

receptor ($CD4^+$) and co-receptor (CXCR4 or CCR5) (1). This viral glycoprotein-

cellular receptor/co-receptor interaction allows entry of HIV through fusion of the

viral envelope with the host cellular membrane; hence endocytosis of the virus.

Upon entry into the host cell, HIV's capsid, which contains its genome ((+) ssRNA) along with viral proteins including reverse transcriptase (also known as RNA-dependent DNA polymerase) and integrase, is released. Once in the host cytoplasm, the viral genome is reversed transcribed from RNA into dsDNA. The dsDNA genome combines with the viral protein integrase and forms the pre-integration complex (PIC). The PIC is imported into the nucleus and the viral genome is integrated into the host genome, which is termed provirus. This HIV-1 provirus is transcribed in the host nucleus using the host machinery. Some transcripts are used as viral genome and others are translated into the viral proteins necessary to produce new virions (1).

Newly synthesized virions are released from the cell and can infect new cells. Once a person gets infected with HIV-1, the virus is present for life; and when left untreated, the viral infection can lead to AIDS (acquired immunodeficiency syndrome). The primary stage of HIV can elicit flu-like symptoms within 2-4 weeks of infection or it may be asymptomatic. This phase can last up to 3 months before HIV-specific antibodies are detected (4). During this phase the virus is infecting cells and replicating.

After this early stage of HIV infection, a strong immune response reduces the number of replicating viruses; and the patient enters the secondary/chronic stage of HIV infection. During this chronic stage, HIV is still actively replicating but reproduction is at a very low level; individuals at this stage may show little to no symptoms (4). However, the disease is still transmissible. If not treated, the chronic

phase can last as little as several weeks or as long as ten or more years. Individuals that go through antiretroviral therapy can remain at this stage for decades.

Individuals that are not treated, overtime, will have severe damage of the immune system, and progression to the third stage of the disease known as AIDS (acquired immunodeficiency syndrome). Individuals with AIDS are susceptible to opportunistic infections, such as infections caused by *Mycobacterium avium*, *Mycobacterium tuberculosis*, *Pneumocystis carinii*, CMV, toxoplasmosis and candidiasis (4).

HIV infection does not have a known cure; however, there are prevention and treatment procedures that have been developed to help lower the risks of getting the virus and to help infected individuals live with the disease. PrEP (pre-exposure prophylaxis) is an effective system of prevention that is based on taking HIV medicines daily and consistently to avoid acquiring the disease. This prevention system has been known to efficiently lower risks of HIV infection through sex or shared injection needles. Once infected with HIV, individuals can go through antiretroviral therapy to lower their viral load (1, 4). This antiretroviral therapy is based on the combination of two or more anti-HIV drugs that may or may not have the same targets depending on the stage of the disease (1).

APOBEC protein family:

Humans encode up to 11 different APOBEC cytidine deaminase proteins including: APOBEC1, APOBEC2, seven APOBEC3s [APOBEC3A (A3A), APOBEC3B (A3B), APOBEC3C (A3C), APOBEC3D (A3D), APOBEC3F (A3F), APOBEC3G (A3G),

and APOBEC3H (A3H)], APOBEC4, and Activation Induced Cytidine Deaminase (AID) (5). The APOBEC enzyme family is thought to be the result of expansion of the ancestral AID gene in the lymphocytes of jawless fish (6). In humans, AID and APOBEC1 (A1) are located on chromosome 12; APOBEC2 (A2) is located on chromosome 6; and the seven APOBEC3 (A3) genes are located in tandem on chromosome 22 (7). APOBEC4 (A4) was the last to be identified and it is located on chromosome 1 (5, 7).

Many of the enzymes from the APOBEC family are DNA cytosine deaminases, and many of the APOBEC3 enzymes were identified to restrict viral invasion through the process of cytosine deamination (8, 9). These cytosine deaminases target different sequences of the genomic DNA for their enzymatic function. AID is known to have a preference for cytosines followed by a purine; A3G is known to have a preference for cytosines followed by another cytosine; A1, A3A/B/C/D/F/H are all known to have a preference for cytosines followed by a thymine; and A2 and A4 are not classified because their activities are as yet unknown (9). APOBEC enzymes are found in many animals such as primates (including humans), mice, cows, sheep, cats, chickens, lizards and fish (9).

The seven APOBEC3 enzymes are structurally related and are composed of either one or two zinc coordinated domains. These domains are structural motifs that contain one or more zinc ions as part of their catalytic core. The APOBEC- type zinc coordinated domains can be subdivided into three groups (A3Z1, A3Z2, and A3Z3) based on their sequence homology (9) (Figure 1). Some of the APOBEC3

family members (A3D, A3F, A3G, and A3H) are potent inhibitors of HIV infection

(10). These APOBEC3 proteins can restrict HIV-1 replication by blocking reverse

transcription of the viral genome to cDNA and through deamination of cytosine to

uracil in nascent retroviral cDNA, which either gets degraded or integrated into the

host genome in its hypermutated form leading the proviral genome to be

nonfunctional (11-13) (Figure 2).

Figure 1: APOBEC conservation among vertebrates. Long arrows represent APOBEC3 enzymes with two zinc-coordinated domains. APOBEC3' enzymes with one zinc coordinated domain are shorter arrows. The zinc coordinated catalytic motifs are represented by different color scheme (green= Z1, yellow= Z2, and purple= Z3). (Figure modified from (9, 12)).
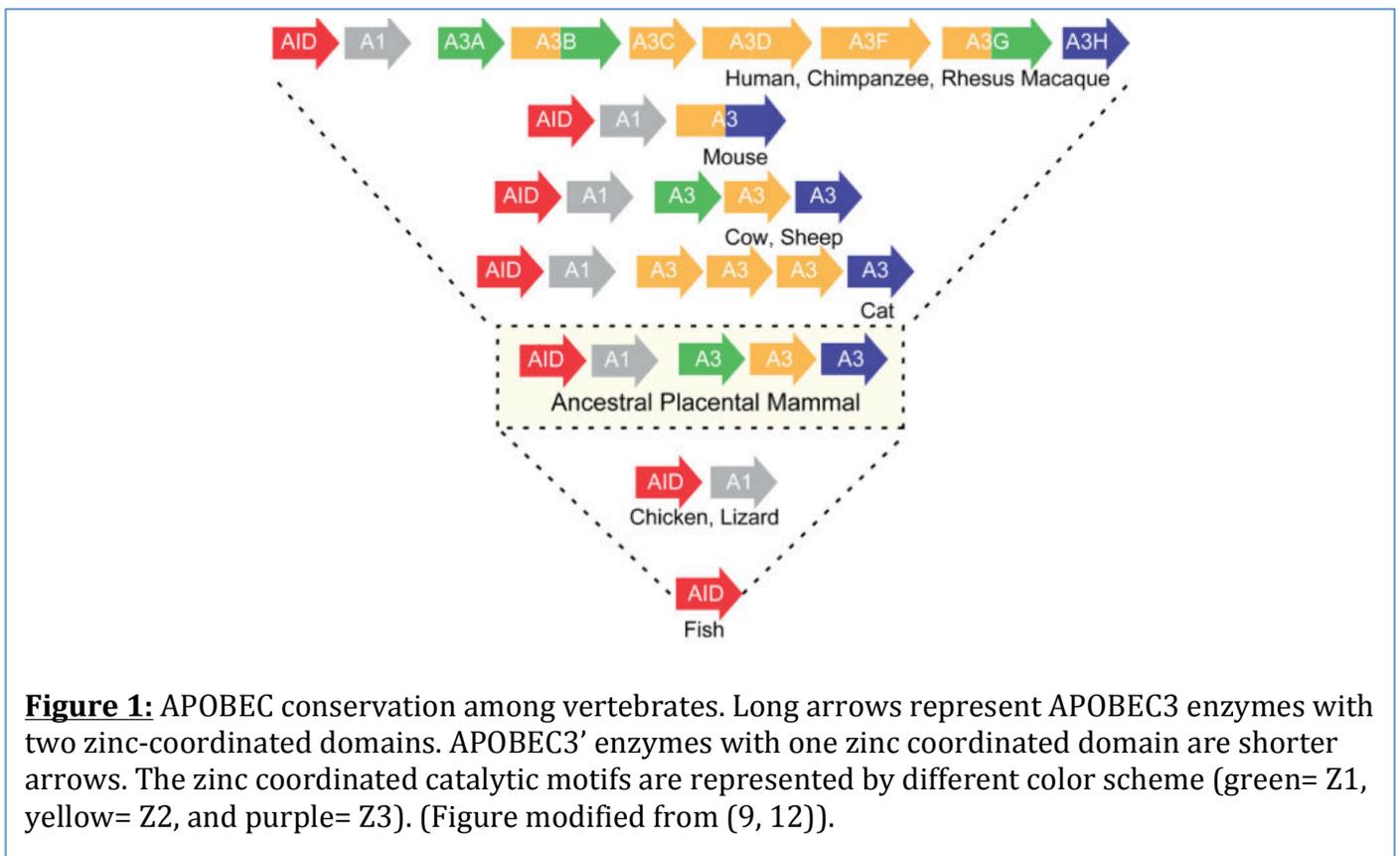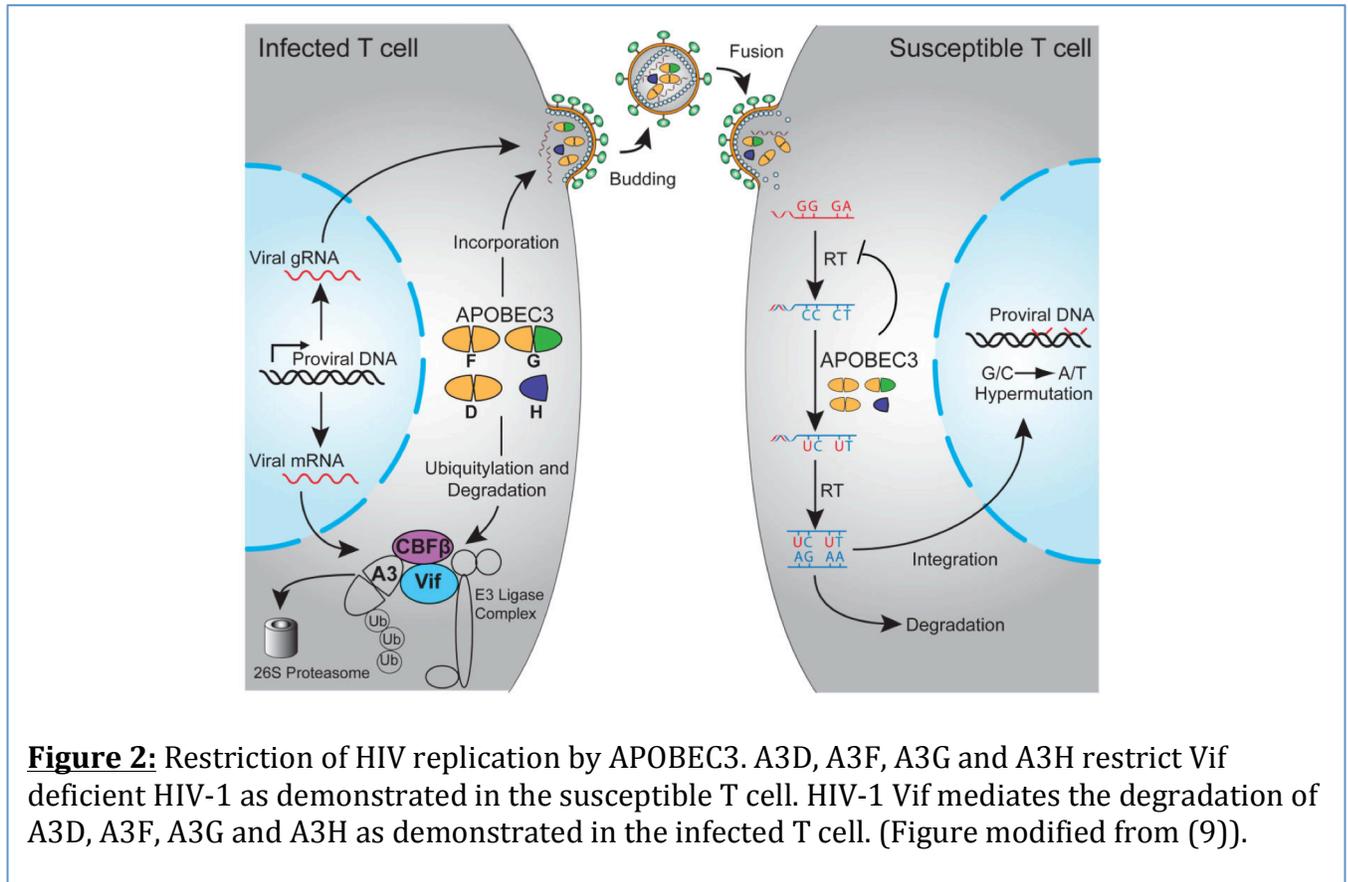
Figure 2: Restriction of HIV replication by APOBEC3. A3D, A3F, A3G and A3H restrict Vif deficient HIV-1 as demonstrated in the susceptible T cell. HIV-1 Vif mediates the degradation of A3D, A3F, A3G and A3H as demonstrated in the infected T cell. (Figure modified from (9)).

Cancer:

The uncontrollable division of cells in the body can lead to cancer. This abnormal cell division can start anywhere in the body and can affect any tissue of the body. The uncontrollable division of cells may develop into masses of tissues known as tumors. These tumors can be benign, in which the cancer does not spread to other tissues or malignant, whereas the cancer spreads to other tissues. Cancer is a genetic disease and there are many factors that lead to its development. These

factors cause changes in the normal function of our genome. One recently described mechanism of tumor diversity and subclonal evolution is DNA cytosine deamination catalyzed by misregulated A3B (Figure 3) (11, 14). A3B was identified as a source of DNA damage and mutagenesis in breast, head/neck, cervix, bladder, lung, ovary, and to lesser extents other cancer types (11, 14, 15). For example, previous studies have demonstrated that A3B mRNAs are overexpressed in most breast tumors and breast cancer cell lines; this was demonstrated by the presence of A3B and cytosine deamination levels that correlate with the genomic uracil levels in cancer genomes (5, 16, 17). This correlation was confirmed through knockdown of endogenous A3B with no cytosine deamination and also with the induction of A3B overexpression in vitro, which results in major DNA damage; leading to C-to-T mutations, cell cycle deviations and cell death(17). Overexpression of A3B in cancer cells can cause mutation clusters or kataegis in the genomic DNA rendering DNA repair difficult (5).

High levels of mutations in cancer tumors (intratumor heterogeneity) are associated with poorer clinical outcomes (11). This intratumor heterogeneity has been determined to be mostly due to enzymatic DNA cytosine deamination by members of the APOBEC family, which were identified as DNA mutators and anti-viral factors (11). These DNA mutators such as A3B, which has been identified as a DNA mutator in many cancers as stated above, could cause genomic instability leading to tumor progression, therefore resistance to cancer therapy (11). In order to identify a tool that could be used to counteract the effects of misregulated A3B in cancer, a lentiviral Vif protein was discovered to mediate the degradation of human

A3B (huA3B) (18). However, it is unlikely that this Vif protein could be delivered to

cancer patients as a whole viral protein, so this interaction needs to be further

characterized before it can be translated to the clinic to help cancer patients.

Figure 3: A3B in cancer progression. Smoking, oncogenic viruses, and sun/UV can cause DNA damage; which may result in the onset of cancer. A3B may increase mutation rates, which can promote tumor evolution. (Image from A.M. Land, unpublished)
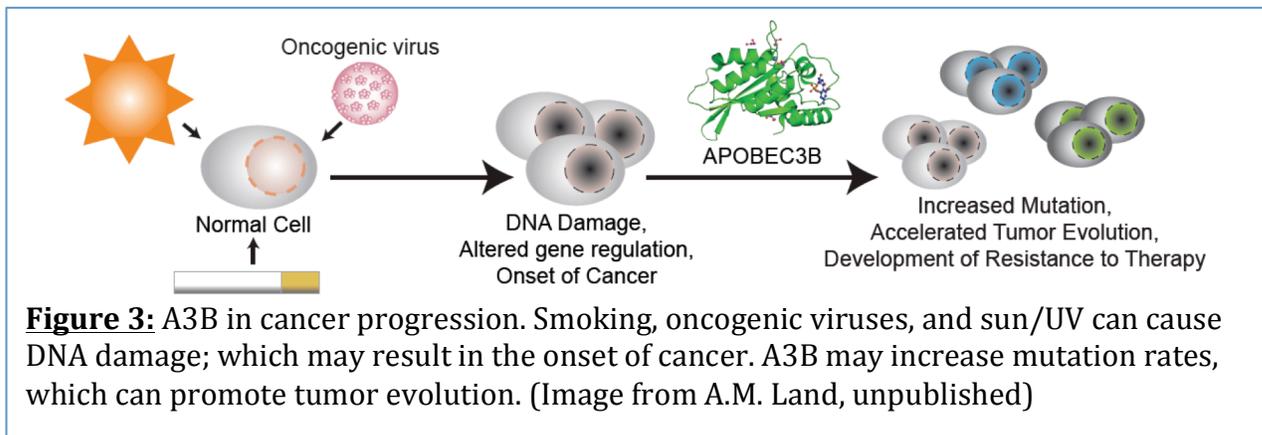
Vif:

HIV-1 encodes the protein Vif (viral infectivity factor), which counteracts the

effect of restrictive APOBEC3 enzymes. This protein mediates the ubiquitination of

APOBEC3 enzymes, targeting them for proteasomal degradation (Figure 4) (8).

The process of HIV-1 Vif mediation of A3G proteasomal degradation is well

described(8). In this degradation cascade, CUL5 (a scaffold protein from the cullin

protein family that inhibits cellular proliferation) directly interacts with EloC (a

component of the Elogin B/C complex, which are protein adaptors) and RBX2 (aka

RING finger protein 2, a regulator for the cascading step for substrate

polyubiquitination), which also interacts with E2 (ubiquitin conjugating enzyme)

(8). The viral Vif protein forms a complex with the host protein CBF- β and A3G. The

complex Vif-CBF-β-A3G interacts with the complex CUL5-EloB/C-RBX2-E2 by binding directly to CUL5 through its zinc-coordinating motif (HCCH) and EloC through its suppressor of cytokines (SOCS box) motif (8). The binding of Vif- CBF-β to CUL5-EloB/C-RBX2-E2 is facilitated by the cofactor CBF-β, which is required for Vif to suppress the antiviral activity of A3G (8). A3G is then polyubiquitinated and targeted for proteasomal degradation (8).

Some other lentiviruses such as HIV-2, SIVmac, SIVagm, SIVcpz, and SIVsmm also encode Vif proteins, which counteract their host species' restrictive APOBEC3 proteins. Additionally, due to the high level of APOBEC3 conservation in primates, Vif-mediated degradation of APOBEC3 proteins can be non-species specific (19). For example, SIVmac is a retrovirus that infects rhesus macaques. It encodes a Vif protein that counteracts human A3B (huA3B) (18). The APOBEC proteins capable of restricting HIV-1 are A3D, F, G and H (10). HIV-1 can counteract these cytosine deaminases by expressing the viral protein Vif (10). The important determinants of A3F, A3G, and A3H for Vif_{HIV-1} and Vif_{HIV-2} mediated degradation have been identified. HIV-1 Vif has been determined to interact with A3G at the β4-α4 loop region, with A3F at the α3 and α4 helices, with A3H at the α3 and α4 helices (13, 20, 21). However, the important determinant of A3D for Vif_{HIV-1} and Vif_{HIV-2} mediated degradation is still being studied (13, 20).

Figure 4: Model of HIV-1 Vif mediated degradation of APOBEC3G. Vif interacts with A3G and initiates a scaffold of protein interactions that leads to A3G ubiquitination and then proteasomal degradation. (Image from (8))
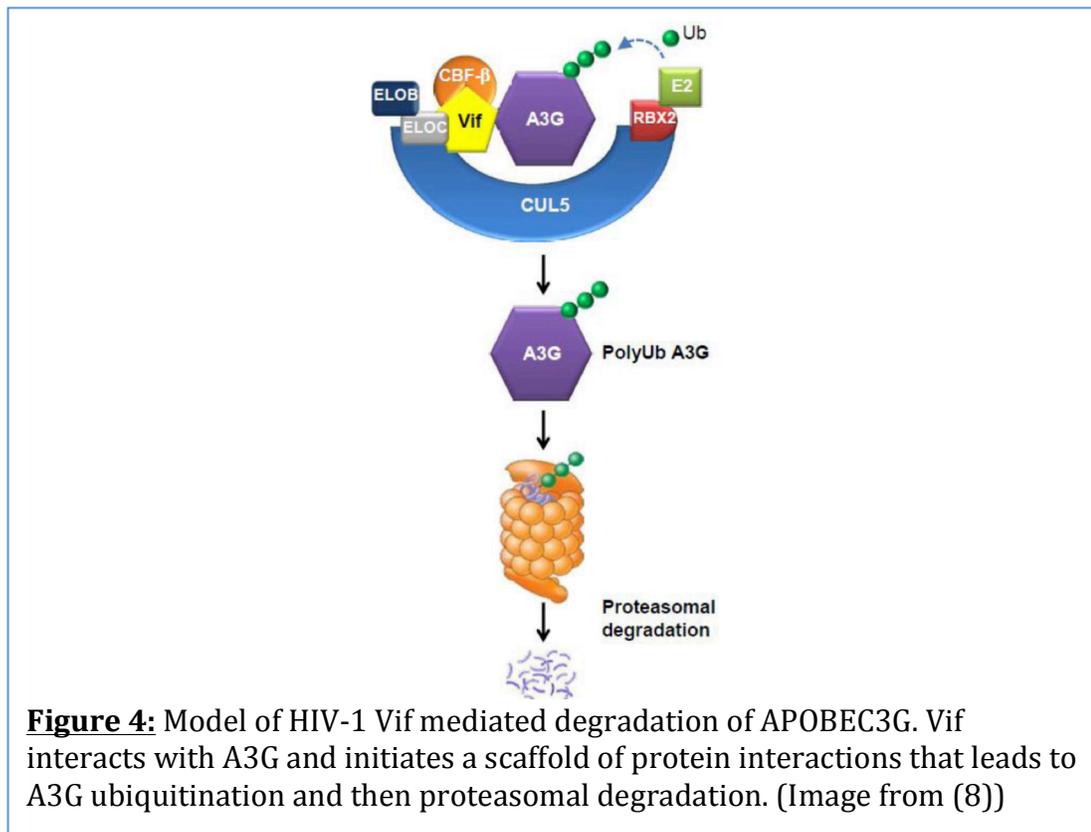
A3B-Vif:

Previous studies have demonstrated that A3B is upregulated in many types of cancer, and that the enzyme plays a major role in cancer diversification (14, 22). As a cytidine deaminase, A3B can deaminate the cytosine base of DNA genomes into uracil (5). Uracil is a non-standard DNA base and must be removed. Repair may lead to errors and genomic mutation. The SIVmac Vif protein has been established to counteract the effect of A3B and therefore is likely to inhibit genomic diversity caused by the presence of misregulated A3B (18). This counteraction of A3B by SIVmac Vif was determined by studying the interactions of multiple lentiviral Vif

proteins with huA3B. The study then revealed SIVmac239 Vif as a potent inhibitor of huA3B (18).

It is important to determine the region on huA3B to which SIVmac Vif binds, in order to characterize the Vif-mediated degradation of huA3B that could lead to the development of SIVmac Vif-based cancer therapies.

Hypothesis and Goal

The goal of this thesis project was to identify the determinants of the interaction between SIVmac Vif and huA3B. A previous study revealed the region of A3F that interacts with HIV-1, which was mapped to be the α3 and α4 helices of huA3F (23). The enzymes from the APOBEC3 family are closely related and similar at both the sequence and structural levels (6). Based on this information, I hypothesized that SIVmac Vif would bind huA3B at a region analogous to where HIV1- Vif interacts with huA3F.

In order to address this goal, a structurally-informed comparison was conducted between huA3B and rhesus A3F (rhA3F), which was previously thought to be resistant to SIVmac Vif-mediated degradation (24). This comparison identified the analogous structural region between huA3B and rhA3F, which identified the region to swap between huA3B and rhA3F.

Next, plasmids expressing huA3B; rhA3F and hA3B/rhA3F chimeras in the same vector backbone were designed using mutagenic primers in site-directed mutagenic PCR. These plasmids were then co-transfected with SIVmac Vif into 293T cells, and degradation of each tested APOBEC3 in the presence of SIVmac Vif was

assessed by immunoblot. I found that SIVmac Vif degraded huA3B and rhA3F, but some of the huA3B/rhA3F chimeras were not degraded by SIVmac Vif protein. I inferred that the α3 and α4 helices in A3F and the α4, α5 and α6 helices in A3B were important for the interaction with SIVmac Vif.

Material and Methods:

I.   Sequence Alignment:

Jalview version 2.10.0b1 and ClustalWS default setting was used to align the amino acid sequences of A3B (Accession number: NM_004900) and A3F (Accession number: NM_001042373) (25). The location of the secondary structure motifs was determined using the crystal structure of huA3B C terminal domain (CTD) (UniProt: Q9UH17) and huA3F CTD (UniProt: Q8IUX4).

II.   Primer Design and Plasmid Construction:

Primers used for plasmids construction were designed following the NEBaseChanger insertion or substitution protocol. Primers were purchased from IDT. The NEB (New England Biolabs) Q5® Site-Directed Mutagenesis Kit Protocol (E0554) was followed for a 25μL PCR reaction. An annealing temperature of 68°C was used for PCR amplification, which was determined using the NEB T_m Calculator (http://tmcalculator.neb.com). *DpnI* was added to each PCR sample after thermocycling. This ensured the digestion of methylated/in vivo synthesized DNA while mutated/in vitro generated DNA stayed intact.

The mutated plasmids were transformed into *Escherichia. coli* (*E. coli*) DHIOB cells following standard protocol and transformants were selected on LB-Amp plates (LB agar+50mg/mL ampicillin). Select clones from the LB-Amp plates were sub-cultured into 2ml LB-Amp broth, which was incubated overnight in a 37°C shaking waterbath.

Plasmids from the selected clones were isolated using the IBI Mini I-Blue Plasmid Kit (IB47172). The eluted products were quantified using a NanoDrop One spectrophotometer, and then digested overnight at 37°C following the restriction enzyme double digestion protocol for *HindIII-HF* (NEB) and *SacII* (NEB). The digested samples were screened for correctly sized products on a 1% agarose gel. Samples that yielded bands of the anticipated sizes were sent to GENEWIZ® (www.genewiz.com) for sequence analysis. The resulting trace files of sequences were interpreted using SEQUENCHER™ version 5.4.1(Gene Codes Coorporation).

Once sequences were confirmed (pcDNA3.1-huA3B-SacII-3xHA and pcDNA3.1-rhA3F-SacII-V5); both plasmids were digested with *HindIII* and *SacII.* The rhA3F open reading frame was purified using the DNA Extraction From Agarose Gels Protocol from the IBI Gel/PCR DNA Fragments Extraction Kit (IB47020); and then subcloned into pcDNA3.1-3xHA plasmid backbone using the NEB Ligation Protocol with T4 DNA Ligase (M0202). The ligated samples were transformed into *E. coli* and selected clones were sub-cultured for plasmids isolation. Plasmids were then screened onto 1% agarose gel to ensure success of ligation.

Chimeric plasmids (huA3B-rha3F α3, and huA3B-rhA3F α4) were created using NEBase Changer Substitution protocol using pcDNA3.1-huA3B-3xHA as a template. Chimeric plasmids (rhA3F-huA3B α4, α5, and rhA3F-huA3B α6) were similarly created using pcDNA3.1-rhA3F-3xHA as a template. Plasmids used for transfection of 293T cells were prepared by transforming them into *E. coli*, culturing single isolated clones into 2mL LB-Amp broth for 6-7 hours, then expanding them

into 200mL LB-Amp broth in a 37°C shaking waterbath overnight. The plasmids were isolated at a high concentration using the IBI Fast Ion Maxi Plasmid Kit Protocol.

III.   Cell Culture

293T cells were propagated in complete DMEM (Dulbecco Modified Eagle Medium), containing 10% FBS (Fetal Bovine Serum) and 100X PenStrep diluted to 1x (10,000 U/mL Penicillin, 10 mg/mL Streptomycin) (VWR LIFE SCIENCE) at 37°C and 5% CO_2. The cells were maintained in 10 cm plates at 10-100% confluency.

IV.   Transfection, Immunoblot and Protein Quantification:

Prior to transfection, 293T cells were counted and 2×10^5 cells were plated into each well of a 6 well plate. After 24 hours, the cells were transfected with different concentrations of APOBEC3 (A3) and Vif expression plasmids (following Table III in appendix) and 8μL of 1 mg/mL PEI (polyethylenimine)(Polysciences Inc)(Figure 5). After 48 hours, the 293T cells were removed from the plates, harvested into microcentrifuge tubes, pelleted, then resuspended and boiled in reducing sample buffer for 20 minutes.

The cell lysates were separated by SDS-PAGE on a 10% polyacrylamide gel (Bio-Rad). The proteins were transferred onto a polyvinylidene difluoride (PVDF) membrane (Immun-Blot® PVDF Membranes for Protein Blotting, Bio-Rad). The membrane was blocked with 4% milk in PBS, probed with a primary antibody (4% milk in PBS-T + 1/1000 rabbit tubulin (GeneTex) + 1/5000 mouse HA (Biolegend) +

azide) overnight at 4°C and then probed with a secondary antibody (4% milk in

PBS-T + 1/10000 goat anti-rabbit tubulin 680 (Life Technologies Alexa Fluor®) +

1/10000 goat anti-mouse HA 800 (IRdye®)+ azide) at room temperature for 1 hour.

Antibody binding was visualized using an infrared ODYSSEY® Fc LI-COR imaging

system. Additionally, ODYSSEY® Fc LI-COR imaging system western analysis was

performed to detect protein bands (A3 and tubulin). Licor densitometry, which

included lane and band adjustments, and protein normalization, was used to

determine the intensity of the A3 and tubulin bands from the immunoblots. A3

protein signal relative to tubulin (tub) was measured as $\frac{A3}{tub}$ for each lane of the

immunoblot. The normalized A3 values were plotted to enable comparison.

Figure 5: Experimental design to determine SIVmac239 Vif mediated-degradation of A3 enzymes after transfection of 293T cells with huAPOBEC3B/rhAPOBEC3F and Vif vectors.
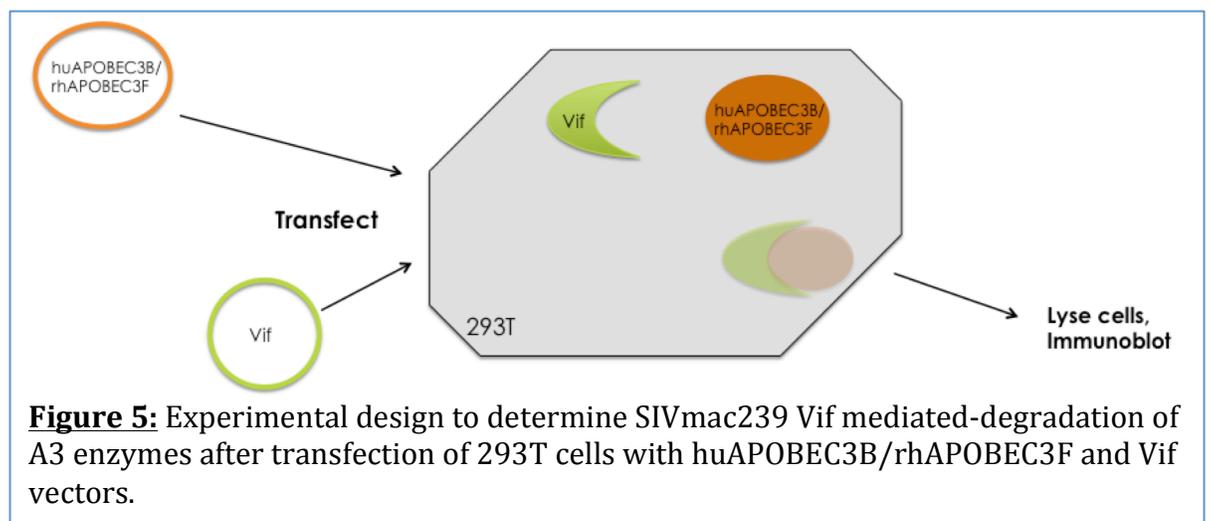
Experimental Results:

I.   Sequence Alignment of huA3B and rhA3F:

In order to compare huA3B (Accession number: NM_004900) and rhA3F (Accession number: NM_001042373), their amino acid sequences were aligned using Jalview software to perform a ClustalWS alignment (25) (Figure 6). The location of the secondary structure motifs was determined based on the crystal structure of huA3B C terminal domain (CTD) (UniProt: Q9UH17) and huA3F CTD (UniProt: Q8IUX4), as the crystal structure of rhA3F has not yet been solved. This alignment demonstrated the amino acid homology between the two enzymes and assisted in the determination of α4, α 5, and α6 regions of huA3B to be analogous to α3 and α4 regions of rhA3F, which is the region bound by HIV-1 Vif (20). This sequence alignment also allowed for the design of the hybrid plasmids that were not predicted to have altered protein folding.
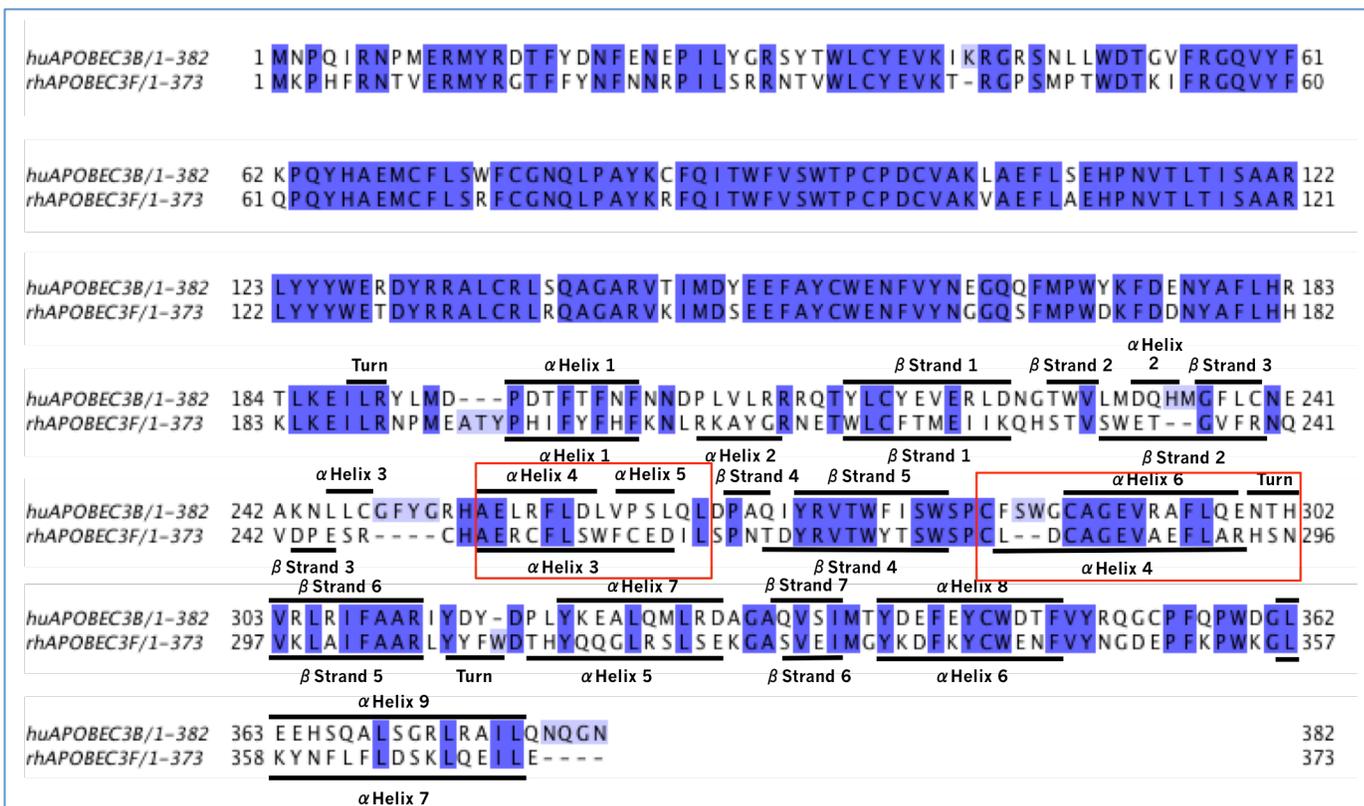
Figure 6: Amino acid sequence alignment of huA3B and rhA3F. The dark color shows where the two sequences have identical amino acids residues. The boxed regions correspond to the region of A3F that interacts with HIV-Vif. These boxed regions also show the analogous regions in huA3B and rhA3F, which are swapped in this project to create chimeric proteins.

II.   Creation of huA3B rhA3F chimeric expression vectors:

The first step to creating the plasmid constructs for this project was to

engineer rhA3F to be expressed with the same epitope tag as huA3B. HuA3B was

originally in a pcDNA3.1 plasmid with 3xHA epitope tag, while rhA3F was in a

pcDNA3.1 plasmid with a V5 epitope tag (Figure 8). pcDNA3.1-3xHA was selected as

the backbone and epitope tag for this experiment, requiring rhA3F to be moved into

pcDNA3.1-3xHA vector. In order to move rhA3F to pcDNA3.1-3xHA, *SacII* restriction

sites (5'CCGC^GG) were created between the C terminus of rhA3F and the V5 epitope tag, and between the C terminus of huA3B and the 3xHA epitope tag to facilitate molecular engineering (Figure 9). This was done by introducing a three-nucleotide insertion of 5'ACC in both plasmids using the NEB Q5 Site-Directed Mutagenesis kit protocol, creating the *SacII* site and keeping the open reading frame of the APOBEC/epitope tag intact (Figure 7). Primers were designed following the NEBaseChanger system in order to perform the mutagenic PCR experiment (see Appendix Table I for primer sequence).
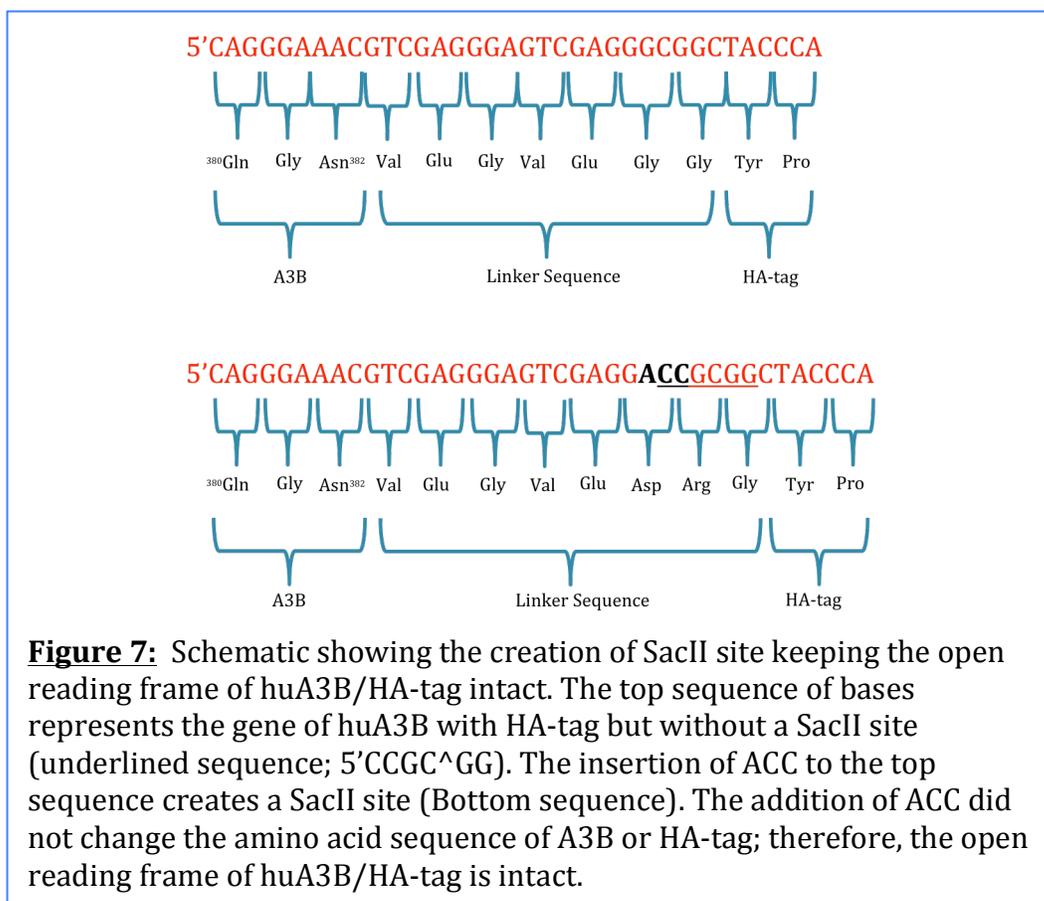
Figure 7: Schematic showing the creation of SacII site keeping the open reading frame of huA3B/HA-tag intact. The top sequence of bases represents the gene of huA3B with HA-tag but without a SacII site (underlined sequence; 5'CCGC^GG). The insertion of ACC to the top sequence creates a SacII site (Bottom sequence). The addition of ACC did not change the amino acid sequence of A3B or HA-tag; therefore, the open reading frame of huA3B/HA-tag is intact.

After the mutagenic PCR, the plasmids were transformed into chemically competent *E. coli*, and screened on LB-Amp plates. Plasmids from select clones were isolated, and the introduction of the *SacII* site was confirmed by restriction digest and by sequence analysis (Figure 10).

The rhA3F open reading frame was subcloned from pcDNA3.1-V5 using *HindIII* (cut site already present) and *SacII* into pcDNA3.1-3xHA. The newly ligated plasmid was transformed and screened on LB-Amp plates. Plasmids from select clones were isolated and the ligation of rhA3F into pcDNA3.1-3xHA was confirmed by restriction digest and sequence analysis (Figure 11).

Figure 8: Parent plasmids of huA3B (pAL008) and rhA3F (pAL012). The top plasmid represents huA3B in a pcDNA3.1-3xHA backbone. The bottom plasmid represents rhA3F in a pcDNA3.1-V5 backbone. Both plasmids already contain an ampicillin resistance gene and a restriction enzyme site for *HindIII* before mutagenic PCR.

Figure 9: HuA3B (pAL029) and rhA3F (pAL030) plasmids with 3xHA epitope tag after mutagenic PCR. The top plasmid represents huA3B in a pcDNA3.1-3xHA that contains an ampicillin resistance gene, and restriction enzyme sites for *HindIII* and *SacII* after mutagenic PCR. The bottom plasmid represents rhA3F now in a pcDNA3.1-3xHA that contains an ampicillin resistance gene, and restriction enzyme sites for *HindIII* and *SacII* after mutagenic PCR.

Figure 10: HuA3B and rhA3F plasmids screened by *HindIII* & *SacII* double digest on an agarose gel after Q5 Site-Directed Mutagenesis. The size of each band is indicated based on 2-log DNA ladder 0.1-10.0Kb (NEB). The parental plasmids for both huA3B and rhA3F were predicted to yield 7.5KB (A3B parent) and 6.5Kb (A3F) bands, while the newly created huA3B and rhA3F were predicted to yield 5.4kb and 21kb (huA3B+SacII), 5.4kb and 1.1kb (rhA3F+SacII) bands.

Figure 11: RhA3F plasmids screened by *HindIII* & *SacII* double digest on an agarose gel after Q5 Site-Directed Mutagenesis and after ligation into pcDNA3.1-3xHA. The size of each band is indicated based on 2-log DNA ladder 0.1-10Kb (NEB). The parental plasmid for rhA3F was predicted to yield a 6.5kb band; while the newly created rhA3F was predicted to yield 5.4kb and 1.1kB bands, and the rhA3F ligated to pcDNA3.1-3xHA was predicted to yield 5.4kb and 1.2kb bands.

In order to create A3B/A3F chimeras, primer-directed mutagenic PCR was performed using plasmids pcDNA3.1-huA3B-3xHA and pcDNA3.1-rhA3F-3xHA to construct a series of A3B/A3F hybrids with the α4, 5 region of A3B swapped with the α3 region of A3F; with the α6 region of A3B swapped with the α4 region of A3F; and where both of these regions were swapped (Figure 12) (see Appendix Table II for plasmids utilized and constructed). In order to create these A3B/A3F hybrids, primers targeting the region to be swapped (amino acids 254 – 302) of huA3B (contains α4, 5, & α6) and (amino acids 250 – 296) of rhA3F (contains α3, & α4) were designed using the NEBaseChanger protocol (Figure 6). The hybrid plasmids were screened by *HindIII* and *SacII* double digest on an agarose gel after primer-directed mutagenic PCR (Figures 13, & 14). Select plasmids were sequenced and sequences were confirmed using the predicted plasmids created using ApE- A plasmid Editor v2.0.49 (http://jorgensen.biology.utah.edu/wayned/ape/) (Figure 15).

Figure 12: HuA3B and rhA3F hybrids constructs. This schematic demonstrates the different chimeras created. The top bars with no insertion of different colored bar (s) represent the parents plasmids with the HA epitope. The other bars with one or two different colored bars insertion represent the different hybrids constructed.
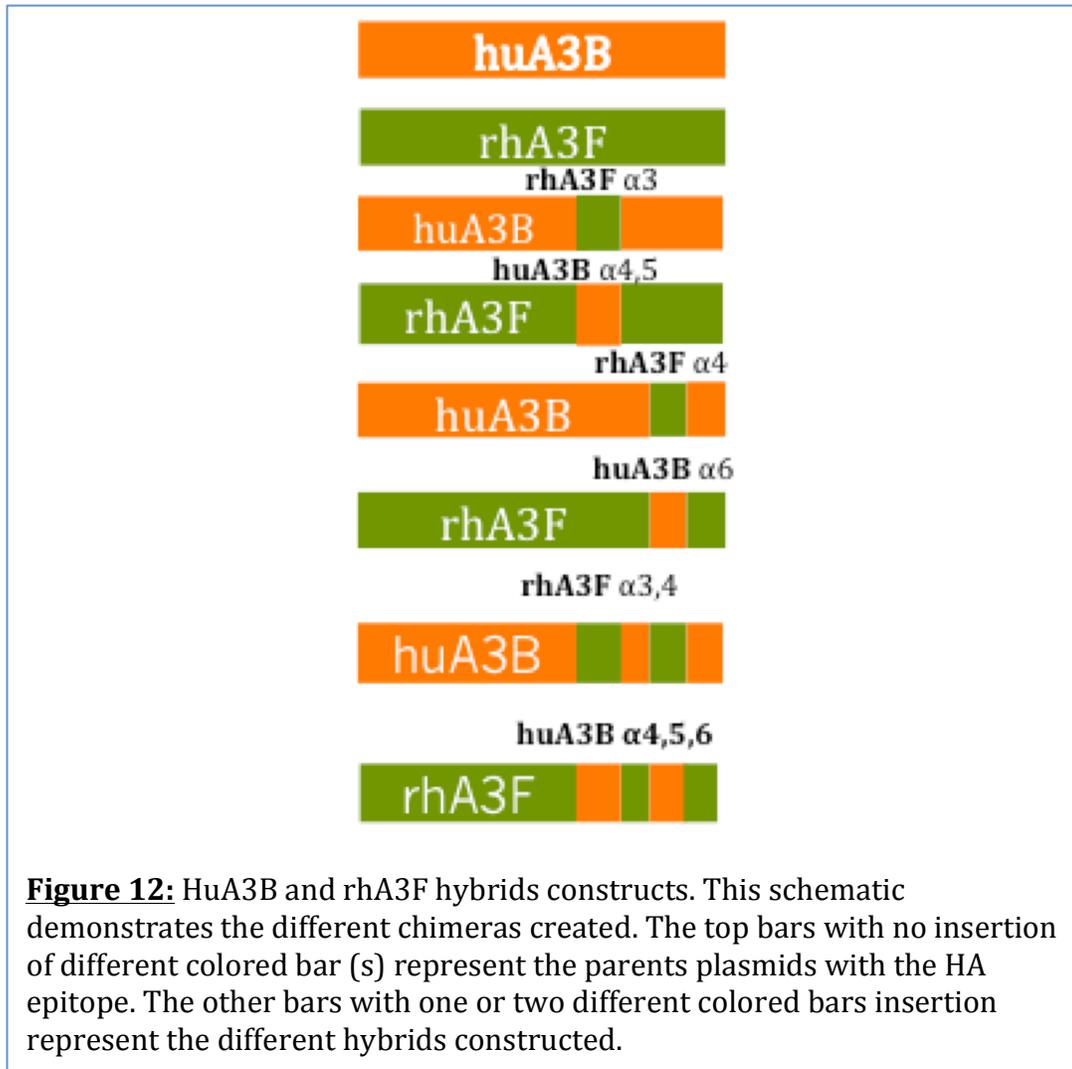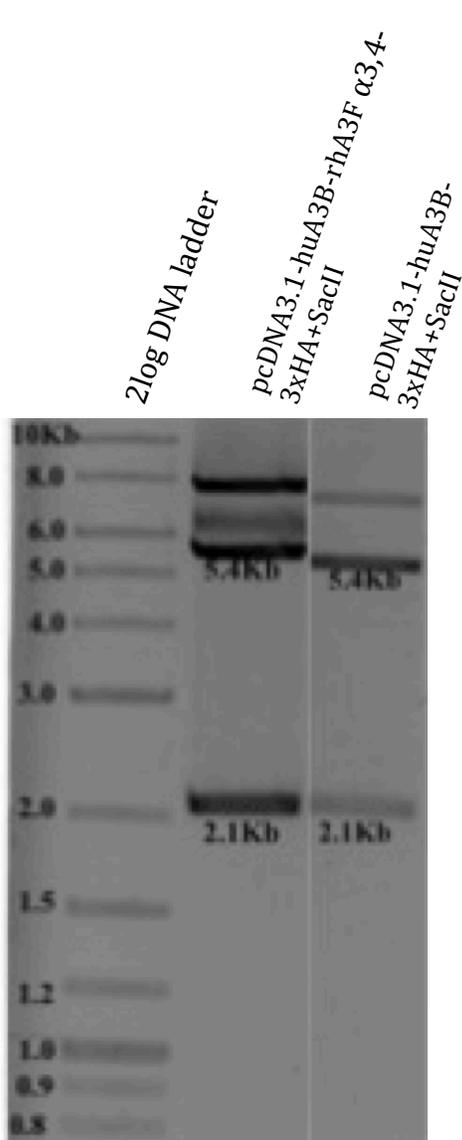
Figure 13: HuA3B hybrid with α 3, 4 helices of rhA3F swapped in and parental huA3B plasmids screened by *HindIII* & *SacII* double digest on an agarose gel after primer-directed mutagenic PCR. The size of each band is indicated based on 2-log DNA ladder 0.1-10kb (NEB). The hybrid huA3B-rhA3F plasmid and huA3B plasmid were both predicted to yield 5.4kb and 2.1kb bands.
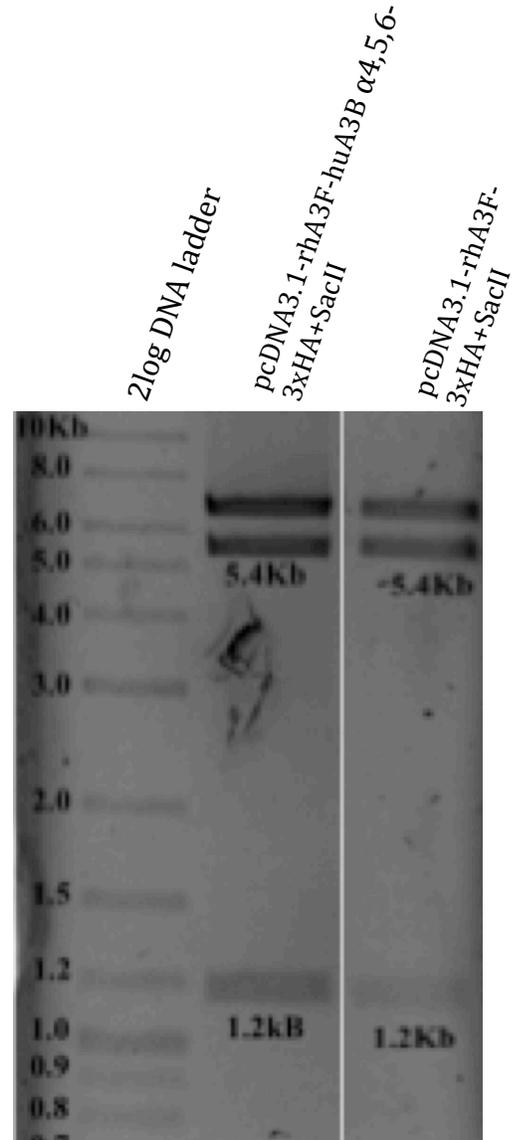
Figure 14: RhA3F hybrid with α 4, 5, 6 helices of huA3B swapped in and parental rhA3F plasmids screened by *HindIII* & *SacII* double digest on an agarose gel after primer-directed mutagenic PCR. The size of each band is indicated based on 2-log DNA ladder 0.1-10kb (NEB). The hybrid rhA3F-huA3B plasmid and rhA3F plasmid were both predicted to yield 5.4kb and 1.2kb bands.
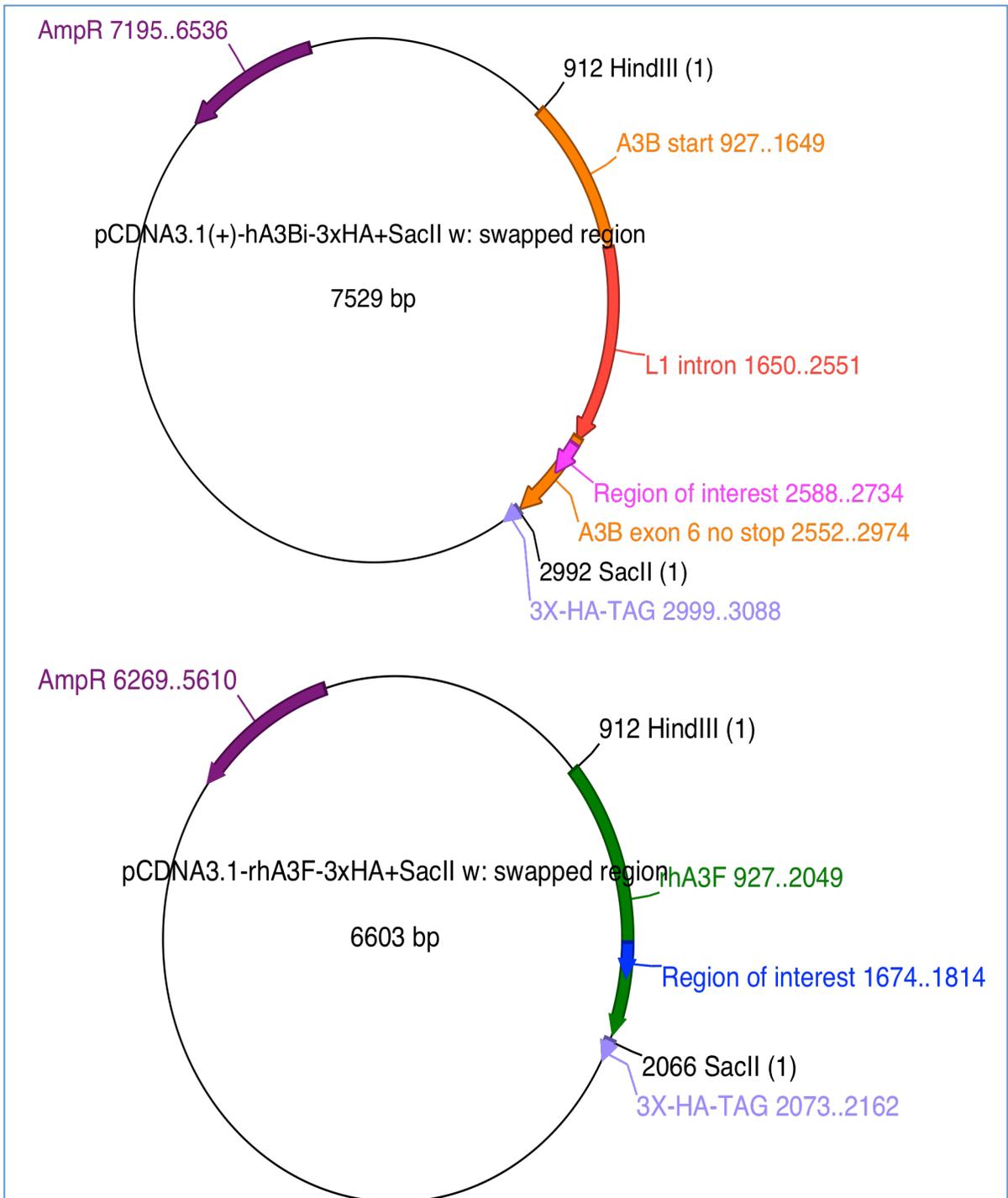
Figure 15: HuA3B and rhA3F with swapped-in regions. The top plasmid represents huA3B in a pcDNA3.1-3xHA that contains an ampicillin resistance gene, restriction enzyme sites for *HindIII* and *SacII*, and a highlighted region of A3B to be swapped out. The bottom plasmid represents rhA3F in a pcDNA3.1-3xHA that contains an ampicillin resistance gene, restriction enzyme sites for *HindIII* and *SacII*, and a highlighted region of A3F to be swapped out.

V. <u>Co-expression of APOBEC and Vif proteins in 293T cells to determine interaction region:</u>

In order to determine the region of interaction between SIVmac239 Vif and huA3B; 293T cells were transfected with hybrids huA3B-rhA3F and SIVmac239 Vif, parents huA3B/rhA3F and SIVmac239 Vif, and with an empty vector and SIVmac239 Vif. Cell lysates were experimentally tested through several immunoblots. Plasmids from the immunoblots were probed and the results are shown below (Figure 16) (see Appendix Table III for transfection conditions).

First, the interaction of huA3B and rhA3F plasmids with SIVmac239 Vif was tested (Figure 16A). 293T cells were transfected with huA3B and SIVmac239 Vif; and with rhA3F and SIVmac239 Vif (see Appendix Table III). 293T cells were also transfected with empty vector and SIVmac239 Vif, which represented our control plasmid for the experiment. No APOBEC3 (No A3) represented the control section on the immunoblot (Figure 16A); and tubulin was used as a loading control to assess transfection. The expression of SIVmac239 Vif in the absence of transfected APOBEC3 proteins was also visualized.

The protein expression levels of both huA3B and rhA3F decreased in the presence low levels of SIVmac239 Vif (Figure 16A). Quantification of the immunoblot revealed a decrease in rhA3F in the presence of low levels of SIVmac239 Vif. However, when the amount of transfected Vif increased; the amount of rhA3F increased, but was lower than rhA3F in the absence of Vif (Figure 16A).

Surprisingly; this result was in direct contrast to the result of SIVmac239 Vif not mediating the degradation of rhA3F stated in a previous report (24). Additionally, quantification of the immunoblot showed a decrease in huA3B in the presence of low levels of SIVmac239 Vif. This result was in agreement with the result of SIVmac239 Vif mediating the degradation of A3B stated in previous literature (18). However, when the amount of transfected Vif increased; the amount of huA3B also increased, but was lower than huA3B in the absence of Vif (Figure 16A).

Next, the sensitivity of huA3B-rhA3F hybrids to Vif-mediated degradation was assessed (Figure 16B). The interaction of the hybrid huA3B-rhA3F α4 plasmid with SIVmac239 Vif was tested by transfecting 293T cells with huA3B-rhA3F α4 and SIVmac239 Vif expression plasmids or empty vector. The protein expression level of huA3B-rhA3F α4, compared to the level of huA3B-rhA3F α4 in the absence of Vif, did not change in the presence of lowest amount of SIVmac239 Vif transfected. Quantification of the immunoblot revealed a higher level of huA3B-rhA3F α4 in the presence of increasing levels of SIVmac239 Vif than huA3B-rhA3F α4 in the absence of Vif (Figure 16B).

The interaction of the hybrid huA3B-rhA3F α3, α4 plasmid with SIVmac239 Vif was also tested by transfecting 293T cells with huA3B-rhA3F α4 and SIVmac239 Vif expression plasmids or empty vector. The immunoblot data showed decreased levels of huA3B-rhA3F α3, α4 in the presence of lowest level of SIVmac239 Vif compared to huA3B-rhA3F α3, α4 in the absence of Vif. Quantification of the immunoblot revealed a higher level of huA3B-rhA3F α3, α4 in the presence of

Figure 16: The interaction of huA3B, rhA3B and huA3B-rhA3F hybrids with SIVmac239 Vif. 293T cells were transfected with huA3B, rhA3F, a huA3B-rhA3F hybrid, or an empty vector (control) and Vif (See Appendix Table III). In each panel the bars over a region of the immunoblot indicate the A3 used in the transfection. The triangles indicate the level of Vif with O representing no Vif added. Quantification of A3 relative to tubulin are shown in the graph below the immunoblot. A. Both huA3B and rhA3F are degraded in the presence of low levels of Vif. Increased level of huA3B and rhA3F are seen with increasing amount of Vif. B. HuA3B-rhA3F α4 is not degraded in the presence of low levels of Vif, while huA3B-rhA3F α3, α4 is degraded in the presence of low levels of Vif. Each A3 shows an increased level of protein with increasing amount of transfected Vif.

increasing levels of SIVmac239 Vif than huA3B-rhA3F α3, α4 in the absence

of Vif (Figure 16B).

Additionally, the interaction of rhA3F with SIVmac239 Vif was tested again

(Figure 16B).

The interaction huA3B-rhA3F α3, rhA3F-huA3B α4, α5, rhA3F-huA3B α6, and

rhA3F-huA3B α4, α5 and α6 hybrids with SIVmac239 Vif were also tested. 293T

cells were transfected with the A3B/rhA3F hybrid and SIVmac239 Vif or vector

control (see Appendix Table III). The result for these assays were inconclusive as

the A3B/A3F hybrid and or Vif was not observed be expressed (data not shown).

Discussion:

The human A3B (huA3B) enzyme is a cytosine deaminase that has the capability to alter the DNA of cancer cells. This change can lead to the evolution of cancer, which consequently can lead to possible resistance to cancer therapy (11, 14, 22). Overexpression of huA3B correlates with high mutation rate in cancer cell lines such as HCC1569, MDA-MB-468, and MDA-MB-453 (17). This high mutation is thought to be caused by the enzymatic activity (deamination of cytosine to uracil) of huA3B in these cancer cell line (17).

SIVmac239 Vif was determined to mediate the degradation of huA3B even though SIV only infects simian primates. Land et al have demonstrated this in a previous study where a decrease in huA3B protein in the presence of increasing amounts of SIVmac239 Vif was observed(18).

The mutations caused by enzymes from the APOBEC3 family are considered to be part of a defense system against viral infections. Viruses have been determined to cause cancer by disrupting cell behavior (DNA damage, mutation in DNA, affect on cell regulation). APOBEC3 enzymes may view the abnormality in cancer DNA as a viral infection and develop a defense system against cancer cells. The human A3B enzyme deaminates cytosine to uracil in the genome of many type of cancers (17). This deamination is thought to cause those cancer types to be resistance to therapy (11). In order to investigate how to halt this resistance of the affected cancer cells my thesis focused on identifying the determinants of the interaction between SIVmac239 Vif and huA3B. This study revealed regions of huA3B that may be

important for interaction, which is a positive step into fulfilling the ultimate goal of developing a therapy to degrade overexpressed huA3B.

I had hypothesized that the region of huA3B analogous to the region of huA3F that interacts with HIV-1, which I determined by sequence alignment to be the α4, 5, and 6 helices, was the region that would interact with SIVmac239 Vif. I first designed huA3B and rhA3F expression constructs in identical vector backbones with the same epitope tag. This experiment allowed the insertion of 5'ACC nucleotides using different pairs of primers for each plasmid in order to create a *SacII* site downstream of each open reading frame (huA3B or rhA3F) but upstream of the epitope tag. Neither plasmid initially contained a recognition site for the *SacII* restriction enzyme; therefore, creating the *SacII* site allowed the enzyme to cut both plasmids only once. Both plasmids initially contained a single recognition site for the *HindIII* restriction enzyme upstream of the open reading frames. The purpose for creating a *SacII* site was to cut the APOBEC3 genes from their vector backbones, and ligate the rhA3F open reading frame to huA3B vector backbone; resulting in both huA3B and rhA3F having pcDNA3.1-3xHA as their vector backbone. This ultimately allowed both constructs to be probed using the same antibody during our immunoblot.

Once the plasmids were successfully created, construction of huA3B hybrid plasmids was initiated using primers specifically designed for the substitution of target regions of huA3B with rhA3F. These target regions, the sequences of huA3B analogous to those of rhA3F that interact with HIV-1, were carefully predicted from

the sequence alignment of huA3B and rhA3F so as to not disrupting protein folding when substituted. The hybrid plasmids were screened on an agarose gel by restriction digest, and sequenced to ensure that there was no additional change in nucleotides sequence besides the substituted regions.

Lastly, transfection experiments were designed to test the interaction of all the A3 proteins with SIVmac239 Vif.

Figure 16A demonstrates that SIVmac239 Vif mediated the degradation of both huA3B and rhA3F. These results were determined as robust A3 expression was observed in the absence of Vif, while A3 protein levels increased with increasing level of SIVmac239 Vif, but not higher than the level of A3 in the absence of Vif. These results illustrate the degradation of A3B in the presence of SIVmac239 Vif, which are in agreement with Land et al(18). However, although a low level of Vif mediates huA3B degradation; higher levels of Vif do not show increased degradation. Interestingly, my results indicated that rhA3F was also sensitive to degradation mediated by SIVmac239 Vif. This is in contrast to the results observed in the study conducted by Virgen et al (24). Additionally, an increase in rhA3F with increasing concentration of SIVmac239 Vif was observed. Possible explanations for rhA3F degradation result include the difference in the experimental methods for transfection. In Virgen et al 293T cells were transfected with a fixed amount of SIVmac239 Vif (150ng) and an increasing amount of rhA3F (75, 150, 300ng), while in my study I transfected 293T cells with higher amount of SIVmac239 Vif (0, 200,

400, 600, and1000ng) relative to a fixed amount of rhA3F (200ng); therefore, degradation may only be observed at specific rhA3F: Vif ratios.

Figure 16B illustrates that SIVmac239 Vif did not interact with huA3B-rhA3F α4, while huA3B-rhA3F α3, α4 interacted with SIVmac239 Vif. The results from the immunoblot showed that both huA3B-rhA3F α4 and huA3B-rhA3F α3, α4 hybrids had robust protein expression in the absence of SIVmac239 Vif. The result from the immunoblot revealed that huA3B-rhA3F with α3, α4 hybrid was only partially degraded in the presence of SIVmac239 Vif as opposed to no Vif. RhA3F α3, α4 is homologous to huA3B α4, α5, and α6, suggesting that this region may be important for SIVmac239 Vif binding to huA3B. HuA3B-rhA3F with α4 hybrid did not get degraded in the presence or absence of SIVmac239 Vif. RhA3F α4 is homologous to huA3B α6, suggesting that this region alone may be important for SIVmac239 Vif binding to huA3B. Overall, these results suggest that the region from residue 289-299 of huA3B that corresponds to α helix 6 may be major determinant of the interaction with SIVmac239 Vif.

Additionally, the quantification of A3 data for all immunoblots revealed an increase in all A3 protein levels with increasing level of SIVmac239 Vif. A possible explanation is that the viral protein SIVmac239 Vif increased in toxicity with increasing concentration. This increased toxicity may have affected cell viability and possibly A3 stability during transfection. However, further studies would be needed to verify this conclusion.

In Wang et al; additional amino acids residues important for the interaction between SIVmac239 Vif and huA3B have been determined (26). The study revealed that the substitution of amino acids [121]RLYYYW[127] in the N terminal domain with alanine residues decreased the degradation of huA3B by SIVmac239 Vif (26). It would be informative to combine the α6 (289-299) residue substitution in this study with the 121-127 residue substitutions from Wang et al and determine if the regions work together to mediate interaction with SIVmac239 Vif.

It is important to understand the molecular basis of the interaction between SIVmac239 Vif-human A3B in order to develop novel cancer therapies to neutralize the effect of huA3B in cancer evolution. This study exploring the site of interaction between SIVmac239 Vif and huA3B is one step closer to identifying huA3B interacting surface of SIVmac239 Vif. This research revealed the regions of huA3B that may be important for interacting with SIVmac239 Vif. This information can be used in future studies focused on the neutralization of APOBEC3 by SIVmac239 Vif.

Appendix:

Table I: Primers used for this project

Primer Name	Primer Sequence	Primer Purpose
1. *SacII* sites in huA3B Forward	ACCGCGGCTACCCATACGATG	Primer pair used to create and amplify a restriction site for *SacII* in pcDNA3.1-huA3B-3xHA (huA3B original plasmid)
2. *SacII* sites in huA3B Reverse	CCTCGACTCCCTCGACGT	
3. *SacII* sites in rhA3F Forward	ACCGCGGCGGTAAGCCTATCC	Primer pair used to create and amplify a restriction site for *SacII* in pcDNA3.1-rhA3F-V5 (rhA3F original plasmid)
4. *SacII* sites in rhA3F Reverse	CCTCGACTCCCTCGACTC	
5. Forward primer α3 (A3F) in A3B	GACATATTGGACCCGGCCCAGATCTACAGGGTCACTTGGTTCATCTCCTGGAGCCCCTG	Primer pair used to substitute α3 helix from pcDNA3.1-rhA3F-3xHA with α4,5 helices of pcDNA3.1-huA3B-3xHA
6. Reverse primer α3 (A3F) in A3B	CTCGCAGAACCAGGAGAGGAAGCACCTTTCTGCATGGCGGCCGTAAAAGCCACAGAGAAGATTCTTAG	
7. Forward primer α4 (A3F) in A3B	GTGGCCGAGTTCCTGGCCAGGCACAGTAATGTGAGACTGCGCATCTTCGCTGCC	Primer pair used to substitute α4 helix from pcDNA3.1-rhA3F-3xHA with α6 helix of pcDNA3.1-huA3B-3xHA
8. Reverse primer α4 (A3F) in A3B	CTCCCCTGCACAATCTAGGCAGGGGCTCCAGGAGATGAACCAAGTGACCCTGTAGATCTG	
9. Forward primer α4, 5 (A3B) in A3F	CAGCTGTCTCCTAACACAGACTACCGGGTCACCTGGTACACATCTTGGAGCCCTTG	Primer pair used to substitute α4,5 helices from pcDNA3.1-huA3B-3xHA with α3 helix of pcDNA3.1-rhA3F-3xHA
10. Reverse primer α4,5 (A3B) in A3F	CAAAGAAGGAACCAGGTCCAAGAAGCGCAGCTCCGCATGACAACGGCTCTCAGGATC	
11. Forward primer α6 (A3B) in A3F	GAAGTGCGTGCGTTCCTTCAGGAGAACACACACGTGAAGCTCGCCATCTTTGCTGCC	Primer pair used to substitute α6 helix from pcDNA3.1-huA3B-3xHA with α4 helix of pcDNA3.1-rhA3F-3xHA
12. Reverse primer α6 (A3B) in A3F	CCCGGCACAGCCCCAGGAGAAGCAAGGGCTCCAAGATGTGTACCAGGTGACCCGGTAG	

Table II: Plasmids used for this project

pAL # (Allison Land plasmid #)	Plasmid Name	Plasmid Identity/Function
pAL008	pcDNA3.1-huA3Bi-3xHA RSH2705	Parent huA3B utilized to create *SacII* site and produce pAL029
pAL012	pcDNA3.1-rhA3F-V5	Parent rhA3F utilized to create *SacII* site and produce pAL028
pAL028	pcDNA3.1-rhA3F-V5+SacII	RhA3F plasmid utilized to produce pAL030
pAL029	pcDNA3.1-huA3Bi-3xHA RSH2705+SacII	Plasmid utilized to produce hybrids of huA3B
pAL030	pcDNA3.1-rhA3F-3xHA RSH2705+SacII	Plasmid utilized to produce hybrids of rhA3F
pAL043	pcDNA3.1-huA3Bi-3xHA RSH2705+SacII+α3 (A3F)	Hybrid huA3B plasmid with rhA3F α3 swap-in
pAL040	pcDNA3.1-rhA3F-3xHA RSH2705+SacII+α4,5 (A3B)	Hybrid rhA3F plasmid with huA3B α4, 5 swap-in
pAL038	pcDNA3.1-huA3Bi-3xHA RSH2705+SacII+α4 (A3F)	Hybrid huA3B plasmid with rhA3F α4 swap-in
pAL039	pcDNA3.1-rhA3F-3xHA RSH2705+SacII+α6 (A3B)	Hybrid rhA3F plasmid with huA3B α6 swap-in
pAL041	pcDNA3.1-huA3Bi-3xHA RSH2705+SacII+α3,4 (A3F)	Hybrid huA3B plasmid with rhA3F α3, 4 swap-in
pAL042	pcDNA3.1-rhA3F-3xHA RSH2705+SacII+α4,5,6 (A3B)	Hybrid rhA3F plasmid with huA3B α4, 5, 6 swap-in

Table III: Transfection Samples Set-Up for this project

Well	Vif	Vif (ng)	A3	A3 (ng)	Vector (ng)	Total (ng)
1	none	0	none	0	1400	1400
2	SIV mac	400	none	0	1000	1400
3	SIV mac	800	none	0	600	1400
4	SIV mac	1200	none	0	200	1400
5	none	0	huA3B	200	1200	1400
6	SIV mac	400	huA3B	200	800	1400
7	SIV mac	800	huA3B	200	400	1400
8	SIV mac	1200	huA3B	200	0	1400
9	none	0	huA3B α4	200	1200	1400
10	SIV mac	400	huA3B α4	200	800	1400
11	SIV mac	800	huA3B α4	200	400	1400
12	SIV mac	1200	huA3B α4	200	0	1400
13	none	0	huA3B α3	200	1200	1400
14	SIV mac	400	huA3B α3	200	800	1400
15	SIV mac	800	huA3B α3	200	400	1400
16	SIV mac	1200	huA3B α3	200	0	1400
17	none	0	huA3B α3, 4	200	1200	1400
18	SIV mac	400	huA3B α3, 4	200	800	1400
19	SIV mac	800	huA3B α3, 4	200	400	1400
20	SIV mac	1200	huA3B α3, 4	200	0	1400
21	none	0	rhA3F	200	1200	1400
22	SIV mac	400	rhA3F	200	800	1400
23	SIV mac	800	rhA3F	200	400	1400
24	SIV mac	1200	rhA3F	200	0	1400
25	none	0	rhA3F α4,5	200	1200	1400
26	SIV mac	400	rhA3F α4,5	200	800	1400
27	SIV mac	800	rhA3F α4,5	200	400	1400
28	SIV mac	1200	rhA3F α4,5	200	0	1400
29	none	0	rhA3F α6	200	1200	1400
30	SIV mac	400	rhA3F α6	200	800	1400
31	SIV mac	800	rhA3F α6	200	400	1400
32	SIV mac	1200	rhA3F α6	200	0	1400
33	none	0	rhA3F α4,5,6	200	1200	1400
34	SIV mac	400	rhA3F α4,5,6	200	800	1400
35	SIV mac	800	rhA3F α4,5,6	200	400	1400
36	SIV mac	1200	rhA3F α4,5,6	200	0	1400

Reference:

1.	Simon V, Ho DD, Abdool Karim Q. 2006. HIV/AIDS epidemiology, pathogenesis, prevention, and treatment. Lancet 368:489-504.
2.	Gopal S, Achenbach CJ, Yanik EL, Dittmer DP, Eron JJ, Engels EA. 2014. Moving forward in HIV-associated cancer. J Clin Oncol 32:876-80.
3.	Sharp PM, Hahn BH. 2011. Origins of HIV and the AIDS pandemic. Cold Spring Harb Perspect Med 1:a006841.
4.	Naif HM. 2013. Pathogenesis of HIV Infection. Infect Dis Rep 5:e6.
5.	Rebhandl S, Huemer M, Greil R, Geisberger R. 2015. AID/APOBEC deaminases and cancer. Oncoscience 2:320-33.
6.	Salter JD, Bennett RP, Smith HC. 2016. The APOBEC Protein Family: United by Structure, Divergent in Function. Trends Biochem Sci 41:578-594.
7.	Vieira VC, Soares MA. 2013. The role of cytidine deaminases on innate immune responses against human viral infections. Biomed Res Int 2013:683095.
8.	Desimmie BA, Delviks-Frankenberrry KA, Burdick RC, Qi D, Izumi T, Pathak VK. 2014. Multiple APOBEC3 restriction factors for HIV-1 and one Vif to rule them all. J Mol Biol 426:1220-45.
9.	Harris RS, Dudley JP. 2015. APOBECs and virus restriction. Virology 479-480:131-45.
10.	Wissing S, Galloway NL, Greene WC. 2010. HIV-1 Vif versus the APOBEC3 cytidine deaminases: an intracellular duel between pathogen and host restriction factors. Mol Aspects Med 31:383-97.
11.	Swanton C, McGranahan N, Starrett GJ, Harris RS. 2015. APOBEC Enzymes: Mutagenic Fuel for Cancer Evolution and Heterogeneity. Cancer Discov 5:704-12.
12.	Hultquist JF, Lengyel JA, Refsland EW, LaRue RS, Lackey L, Brown WL, Harris RS. 2011. Human and rhesus APOBEC3D, APOBEC3F, APOBEC3G, and APOBEC3H demonstrate a conserved capacity to restrict Vif-deficient HIV-1. J Virol 85:11220-34.
13.	Letko M, Booiman T, Kootstra N, Simon V, Ooms M. 2015. Identification of the HIV-1 Vif and Human APOBEC3G Protein Interface. Cell Rep 13:1789-99.
14.	Kuong KJ, Loeb LA. 2013. APOBEC3B mutagenesis in cancer. Nat Genet 45:964-5.
15.	Harris RS. 2015. Molecular mechanism and clinical impact of APOBEC3B-catalyzed mutagenesis in breast cancer. Breast Cancer Res 17:8.
16.	Zou J, Wang C, Ma X, Wang E, Peng G. 2017. APOBEC3B, a molecular driver of mutagenesis in human cancers. Cell Biosci 7:29.
17.	Burns MB, Lackey L, Carpenter MA, Rathore A, Land AM, Leonard B, Refsland EW, Kotandeniya D, Tretyakova N, Nikas JB, Yee D, Temiz NA, Donohue DE, McDougle RM, Brown WL, Law EK, Harris RS. 2013. APOBEC3B is an enzymatic source of mutation in breast cancer. Nature 494:366-70.

18.   Land AM, Wang J, Law EK, Aberle R, Kirmaier A, Krupp A, Johnson WE, Harris RS. 2015. Degradation of the cancer genomic DNA deaminase APOBEC3B by SIV Vif. Oncotarget 6:39969-79.

19.   LaRue RS, Andresdottir V, Blanchard Y, Conticello SG, Derse D, Emerman M, Greene WC, Jonsson SR, Landau NR, Lochelt M, Malik HS, Malim MH, Munk C, O'Brien SJ, Pathak VK, Strebel K, Wain-Hobson S, Yu XF, Yuhki N, Harris RS. 2009. Guidelines for naming nonprimate APOBEC3 genes and proteins. J Virol 83:494-7.

20.   Land AM, Shaban NM, Evans L, Hultquist JF, Albin JS, Harris RS. 2014. APOBEC3F determinants of HIV-1 Vif sensitivity. J Virol 88:12923-7.

21.   Nakashima M, Tsuzuki S, Awazu H, Hamano A, Okada A, Ode H, Maejima M, Hachiya A, Yokomaku Y, Watanabe N, Akari H, Iwatani Y. 2017. Mapping Region of Human Restriction Factor APOBEC3H Critical for Interaction with HIV-1 Vif. J Mol Biol 429:1262-1276.

22.   Burns MB, Temiz NA, Harris RS. 2013. Evidence for APOBEC3B mutagenesis in multiple human cancers. Nat Genet 45:977-83.

23.   Richards C, Albin JS, Demir O, Shaban NM, Luengas EM, Land AM, Anderson BD, Holten JR, Anderson JS, Harki DA, Amaro RE, Harris RS. 2015. The Binding Interface between Human APOBEC3F and HIV-1 Vif Elucidated by Genetic and Computational Approaches. Cell Rep 13:1781-8.

24.   Virgen CA, Hatziioannou T. 2007. Antiretroviral activity and Vif sensitivity of rhesus macaque APOBEC3 proteins. J Virol 81:13932-7.

25.   Waterhouse AM PJ, Martin DMA, Clamp M, Barton GJ. 2009. Jalview Version 2-a multiple sequence alignment editor and analysis workbench, vol 25, p 1189-1191, Bioinformatics.

26.   Wang J, Shaban NM, Land AM, Brown WL, Harris RS. 2018. Simian Immunodeficiency Virus Vif and Human APOBEC3B Interactions Resemble Those between HIV-1 Vif and Human APOBEC3G. J Virol 92.